

*Observation and appearance of magnetospheric
instability in flaring activity at the onset of X-
ray outbursts in A 0535+26*

K A .Postnov (SAI)

In collaboration with:

*R Staubert, A Santangelo, P Kretschmar,
I Caballero, D Kubchikov
IAAT, U .of Tuebingen*

Introduction

A0535+26

Transient Be/X-ray binary

- Type II outbursts (giant), $L_X > 10^{37} \text{ erg ss}^{-1}$
- Type I (normal), associated with periastron, $L_X \sim 10^{36-37} \text{ erg ss}^{-1}$
- quiescence states, persistent low luminosity, $L_X \lesssim 10^{36} \text{ erg ss}^{-1}$

Discovered in 1975 during a giant outburst (Rosenberg et al. 1975)

Neutron star

- $P_{\text{spin}} \sim 103 \text{ s}$
- $B \sim 4 \times 10^{12} \text{ G}$
- $R \sim 10 \text{ km}, M \sim 1.4 M_\odot$
- $P_{\text{orb}} = 111 \text{ days}, e = 0.47$
- $d \sim 2 \text{ kpc}$

HDE 245770 - O9.7, IIIe

- $14 M_\odot, 14 R_\odot$
- $1.41 \times 10^5 L_\odot$
- $T_{\text{eff}} = 26000 \text{ K}$

Review: Giovannelli & Graziati 1992

Transient Source

The source has shown 5 giant outbursts since its discovery

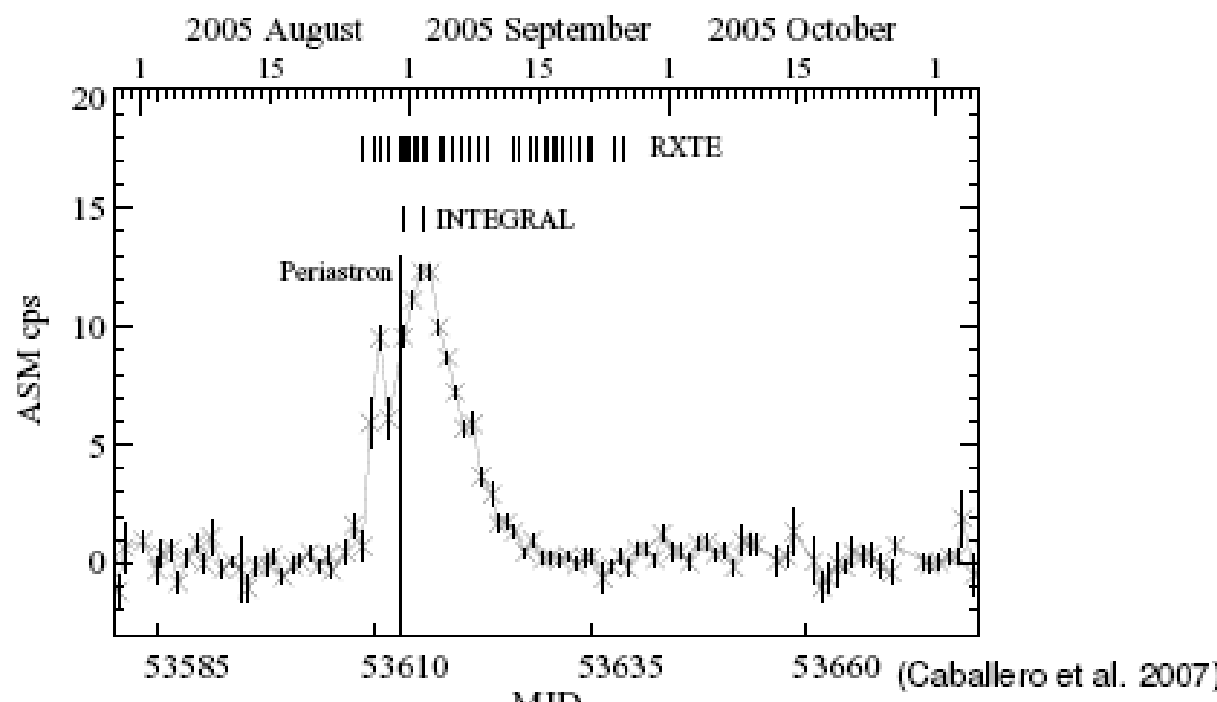
- April/May 1975 - $L_{(3-50\text{keV})} \sim 1.2 \times 10^{37}\text{ergss}^{-1}$
(Rosenberg et al. 1975)
- October 1980 - $L_{(1-22\text{keV})} \sim 3 \times 10^{37}\text{ergss}^{-1}$
(Nagase et al. 1982)
- June 1983 - $L_{(32-91)\text{keV}} \sim 2 \times 10^{37}\text{ergss}^{-1}$
(Sembay et al. 1990)
- March/April 1989 - $L_{(23-52\text{keV})} \sim 1.3 \times 10^{37}\text{ergss}^{-1}$
(Makino et al. 1989)
- February 1994 - $L_{(20-40\text{keV})} \sim 3.6 \times 10^{37}\text{ergss}^{-1}$
(Finger et al. 1994)
- May/June 2005 - $L_{(15-195\text{keV})} \sim 4.8 \times 10^{37}\text{ergss}^{-1}$
(Tueller et al. 2005)

Too close to the sun to be observed!!

Transient Source

From 1994 until 2005 it has been in quiescence.

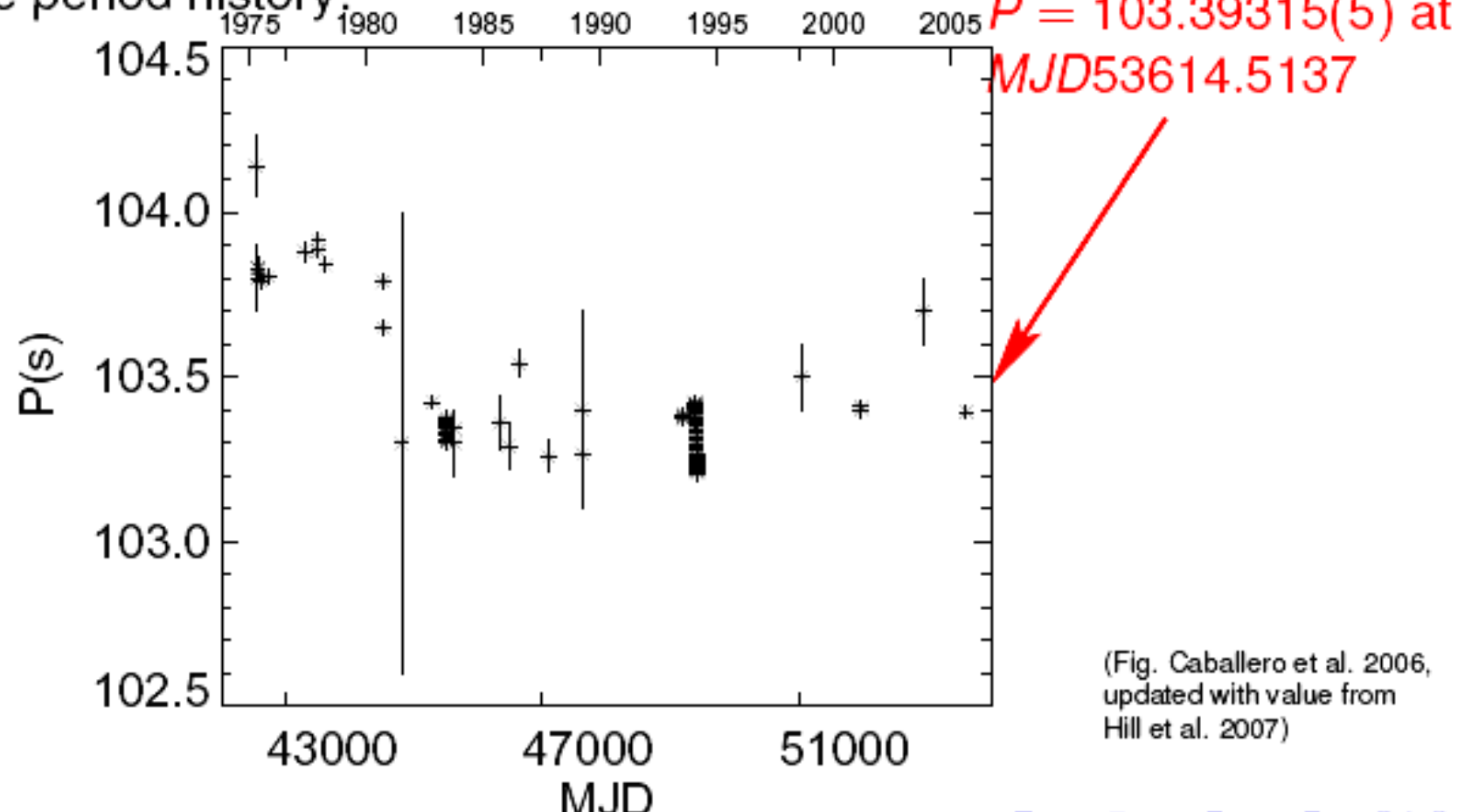
- May/June 2005: giant outburst, $L_{(15-195\text{keV})} \sim 4.8 \times 10^{37} \text{ergss}^{-1}$ (Tueller et al. 2005)
- Aug/Sept 2005: normal outburst, $L_{(15-195\text{keV})} \sim 0.6 \times 10^{37} \text{ergss}^{-1}$
- December 2005: normal outburst $L_{(15-195\text{keV})} \sim 0.2 \times 10^{37} \text{ergss}^{-1}$



Timing: pulse period search with INTEGRAL

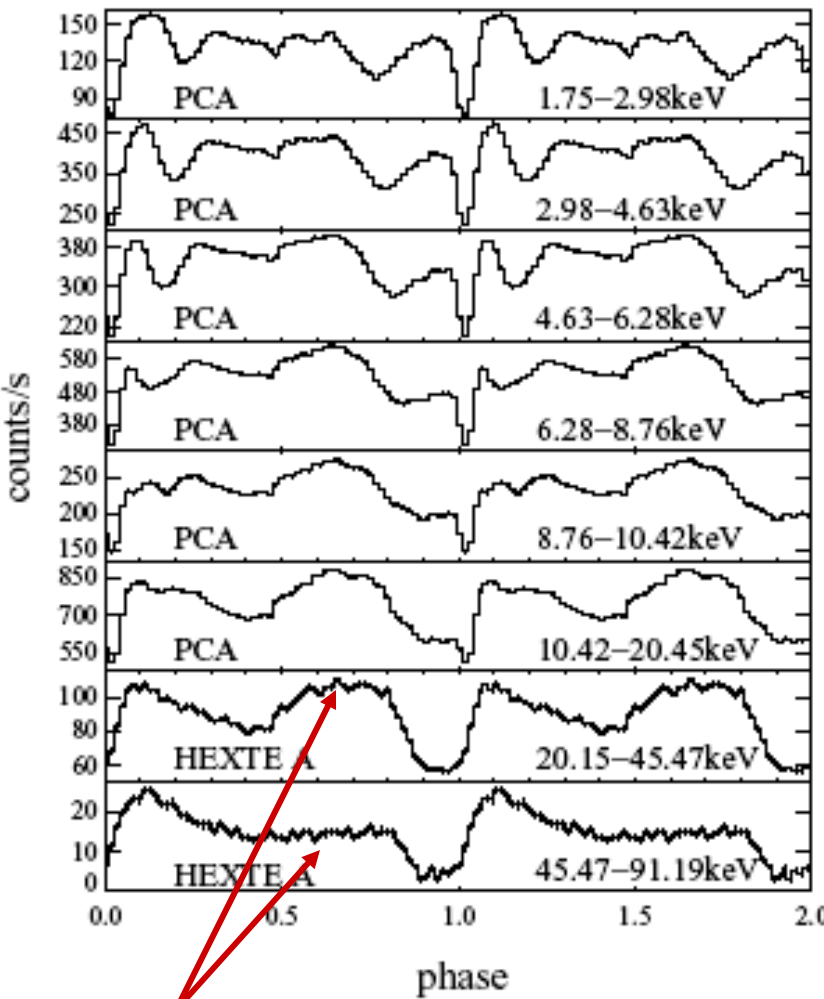
Pulse period determined with high accuracy using IBIS-ISGRI data.

Pulse period history:

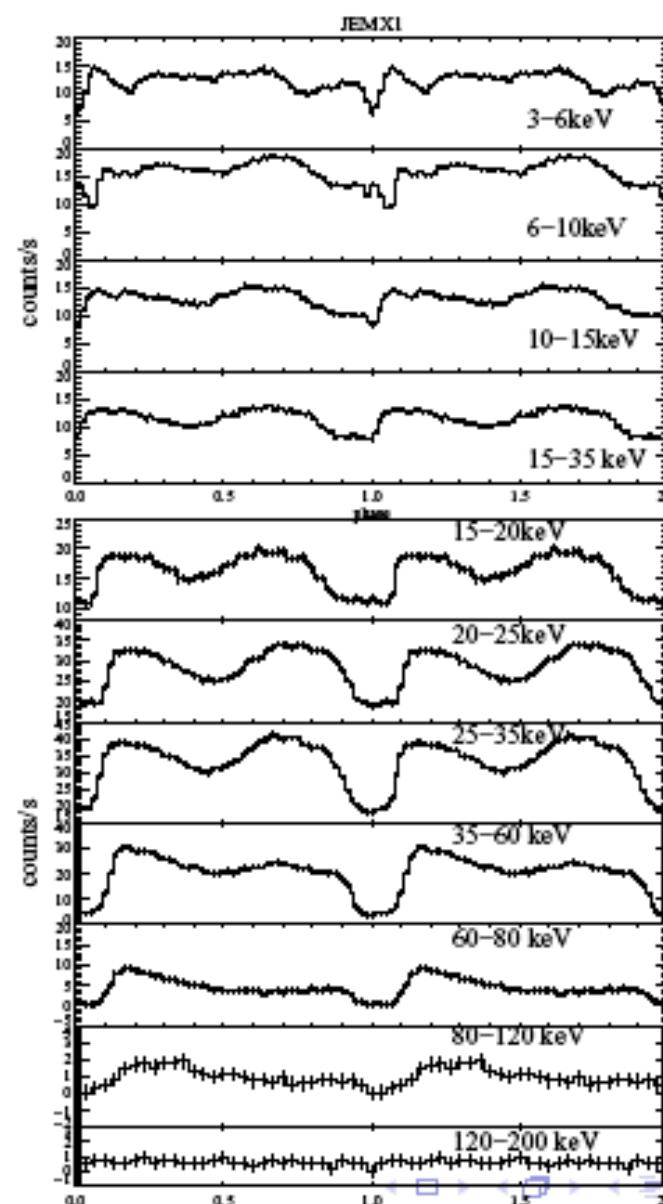


Timing: energy dependent pulse profiles

RXTE



INTEGRAL



JEMX-1

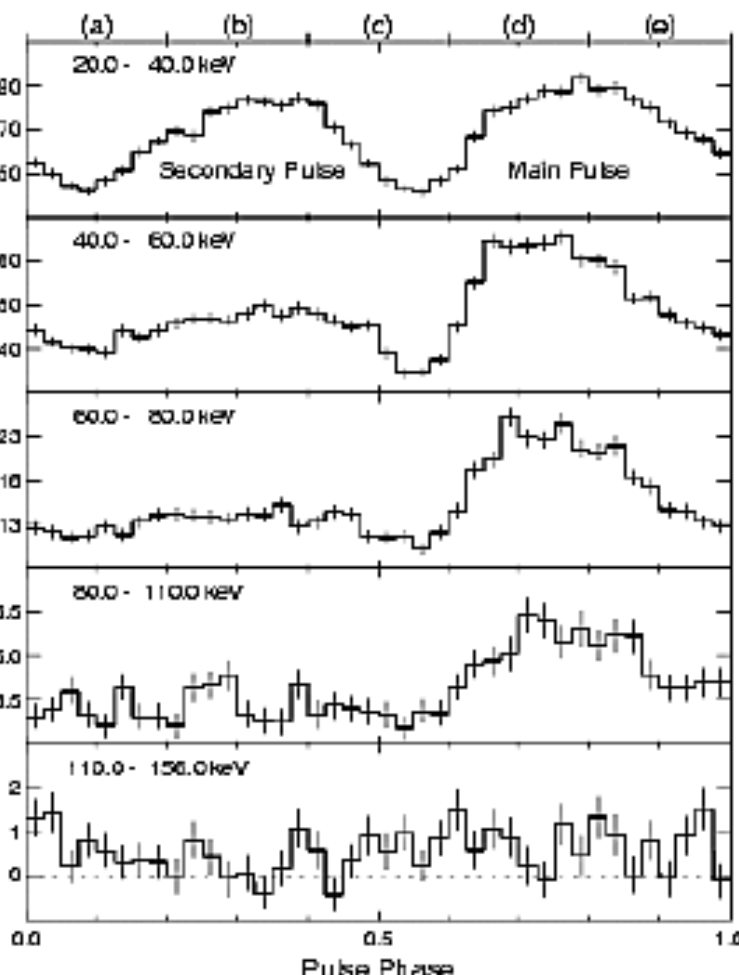
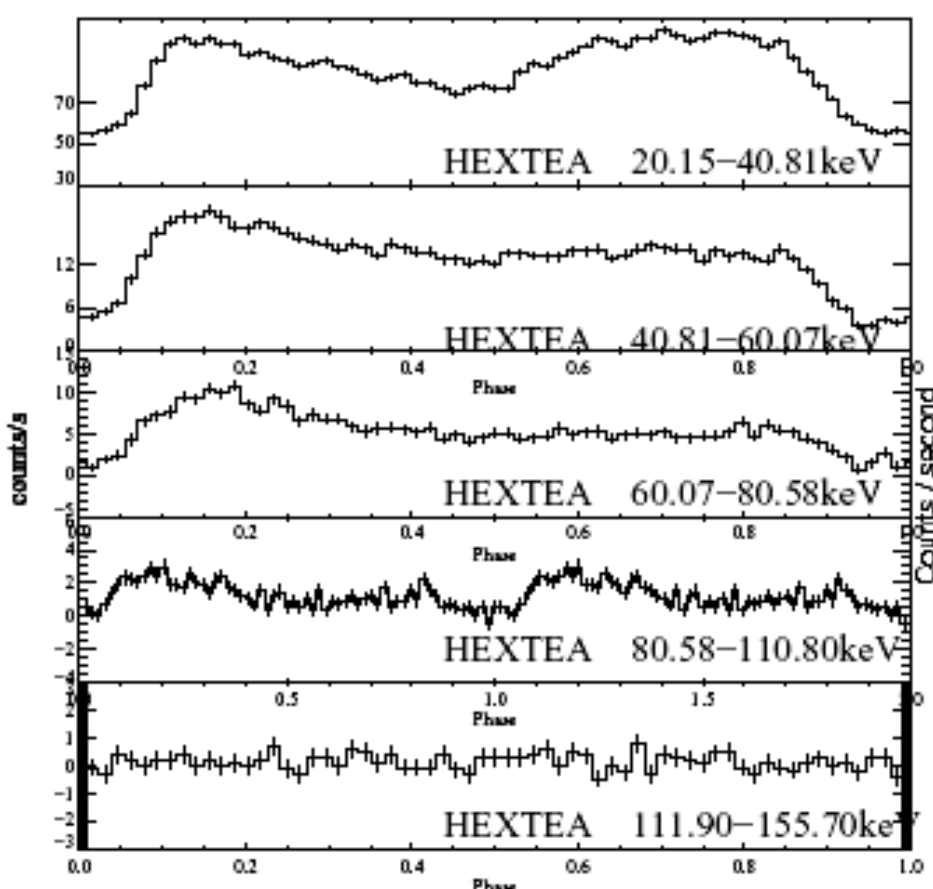
IBIS

Timing: energy dependent pulse profiles

August/Sept.2005 normal outburst

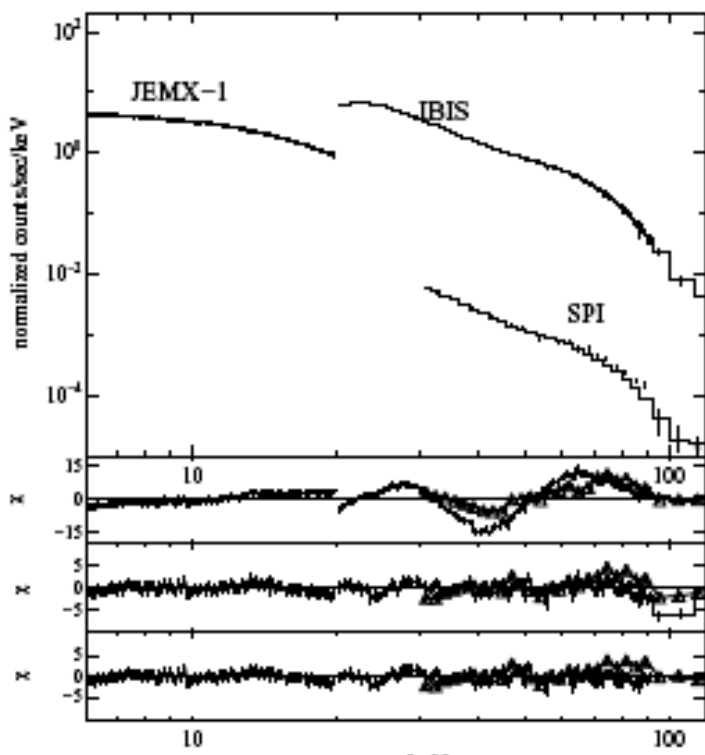
$$L(23 - 53\text{keV}) \sim 0.23 \times 10^{37} \text{ergs}^{-1}$$

March/April 1989 giant outburst
 $L(23 - 53\text{keV}) \sim 1.26 \times 10^{37} \text{ergs}^{-1}$
TTM/HEXE observations (Kendziorra et al. 1994)



X-ray spectra: fundamental cyclotron line at 45keV

INTEGRAL

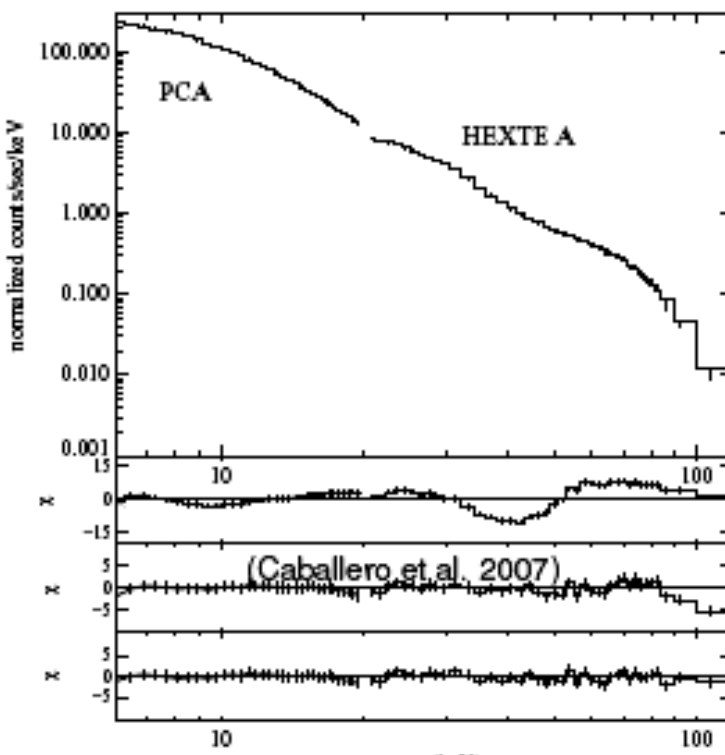


$$E_1 = 45.9^{+0.3}_{-0.3} \text{ keV}$$

$$E_2 = 102^{+4}_{-3} \text{ keV}$$

$$E_{cyc} = 11.6 \text{ keV} B \times 10^{12} \text{ G} \Rightarrow B \sim 4 \times 10^{12} \text{ G}$$

RXTE



$$E_1 = 45.9^{+0.4}_{-0.3} \text{ keV}$$

$$E_2 = 103^{+3}_{-3} \text{ keV}$$

Result confirmed by Suzaku (Terada et al. 2006): $E_1 = 46.3 \pm 1.5 \text{ keV}$

X-ray spectra: Cyclotron line evolution with luminosity

super-Eddington regime

High accretion rates

Shock formation in accretion column

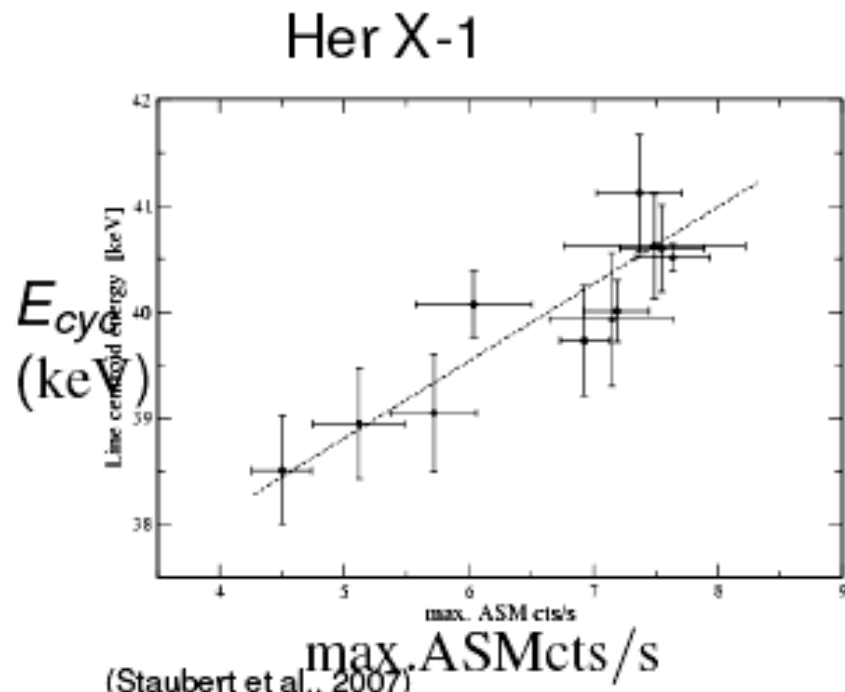
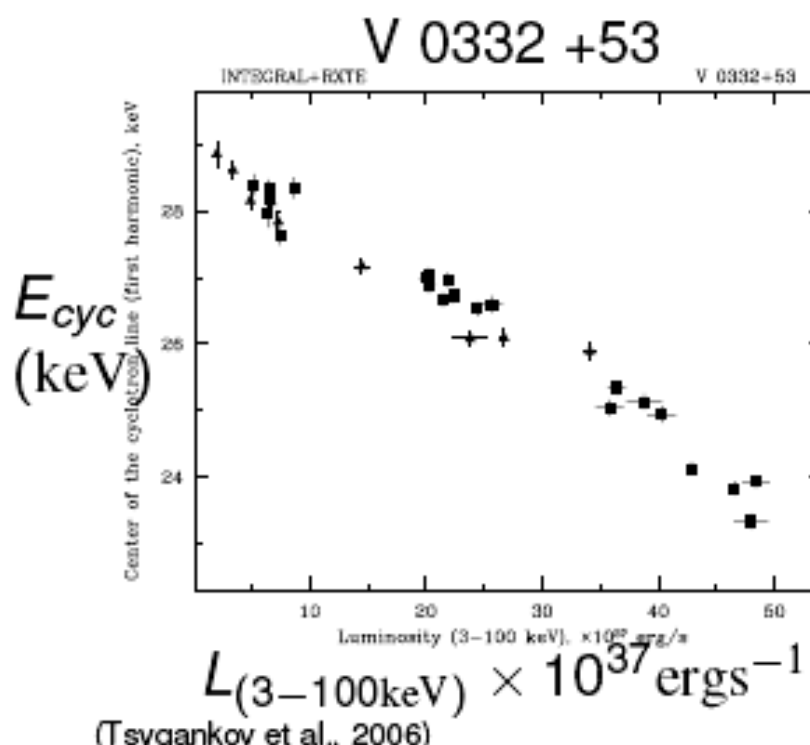
Height of shock $\propto \dot{m}$

sub-Eddington regime

Low accretion rates

No shock is formed

(Basko & Sunyaev 1976)



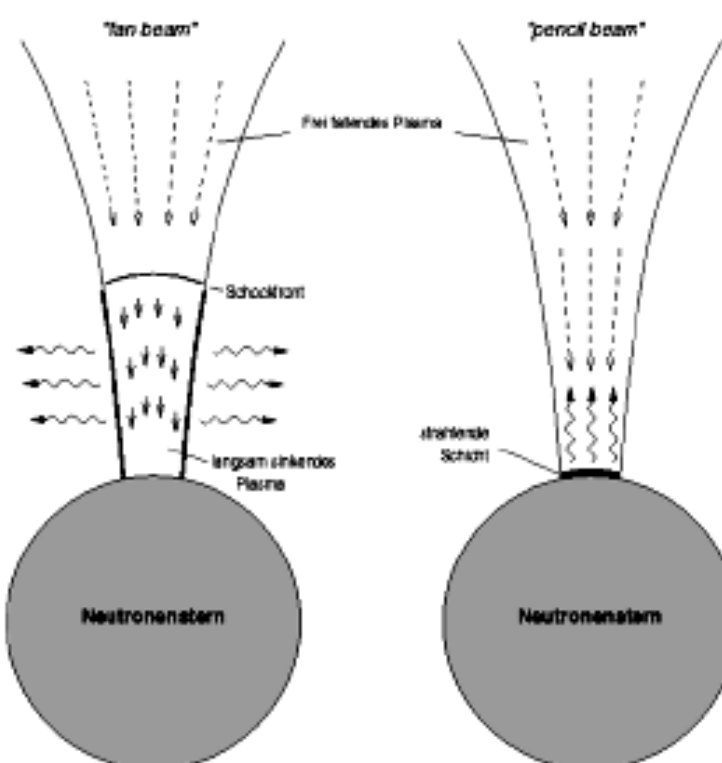
Accretion columns

Matter forced to follow the B field lines.

Extreme physical conditions in the accretion funnel:

- $B \sim 10^{12}$ G
- relativistic plasma
- $L \sim L_{Edd}$

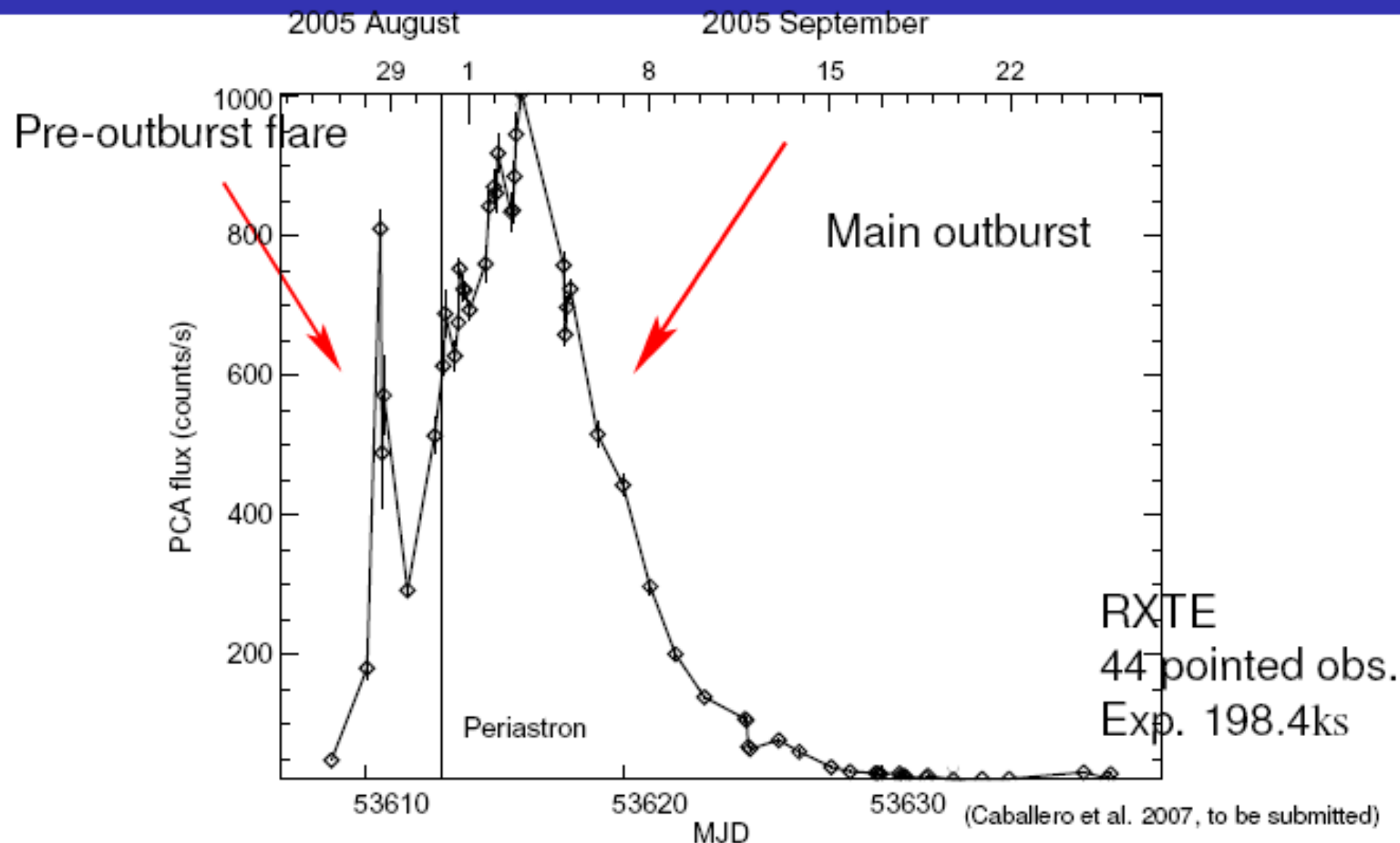
High accretion rates



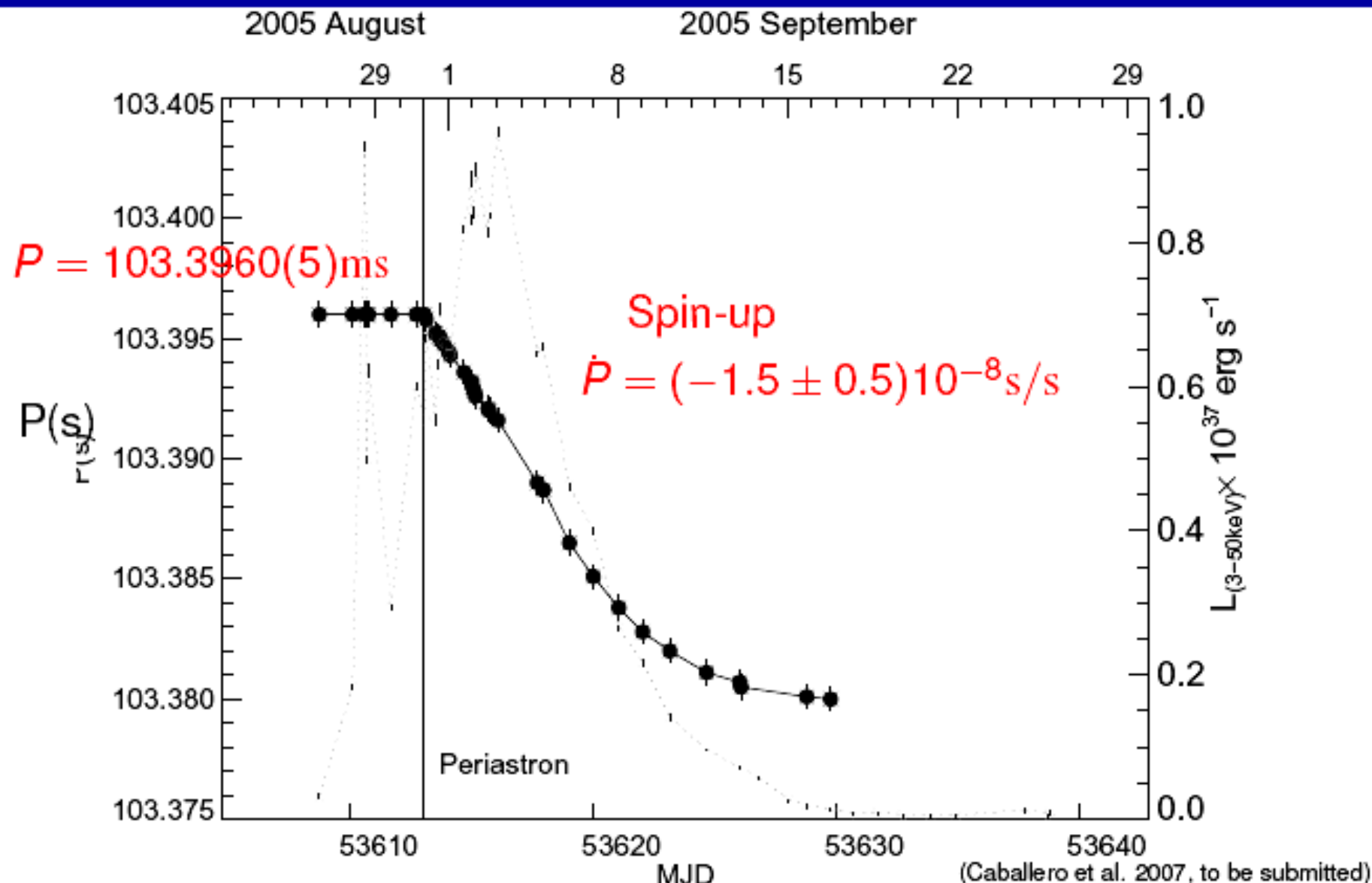
Low accretion rates

(Kretschmar, 1996 after Harding, 1994)

Evolution of timing and spectral parameters during the outburst - RXTE

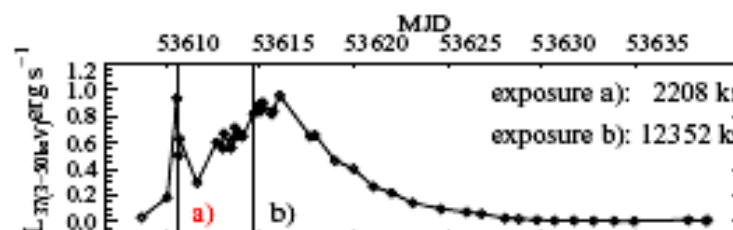


Pulse period evolution



Pulse profiles evolution

Strong variation of energy dependent pulse profiles



a) FLARE

b) NEAR MAXIMUM

PCA 1.75 – 2.98keV

PCA 2.98 – 4.63keV

PCA 4.63 – 6.28keV

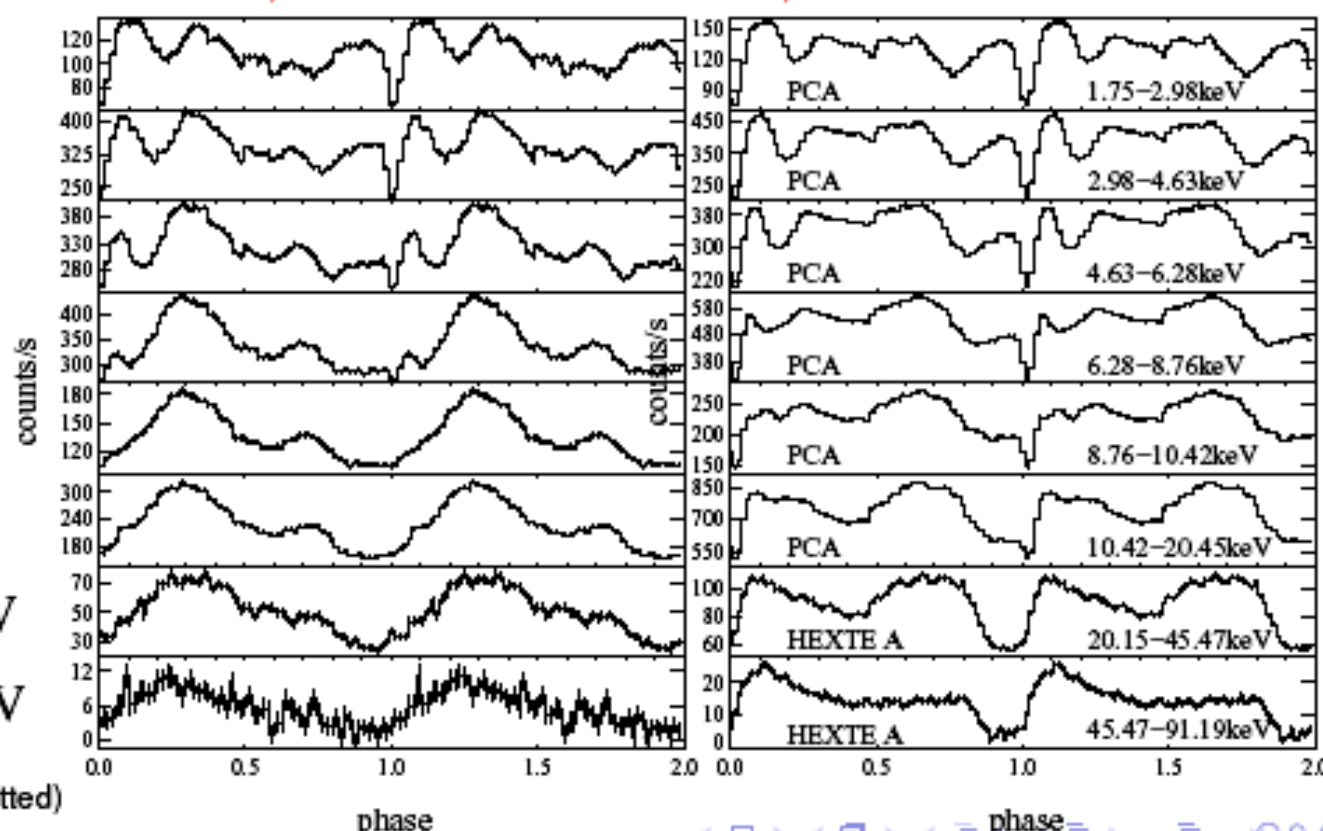
PCA 6.28 – 8.76keV

PCA 8.76 – 10.42keV

PCA 10.42 – 20.45keV

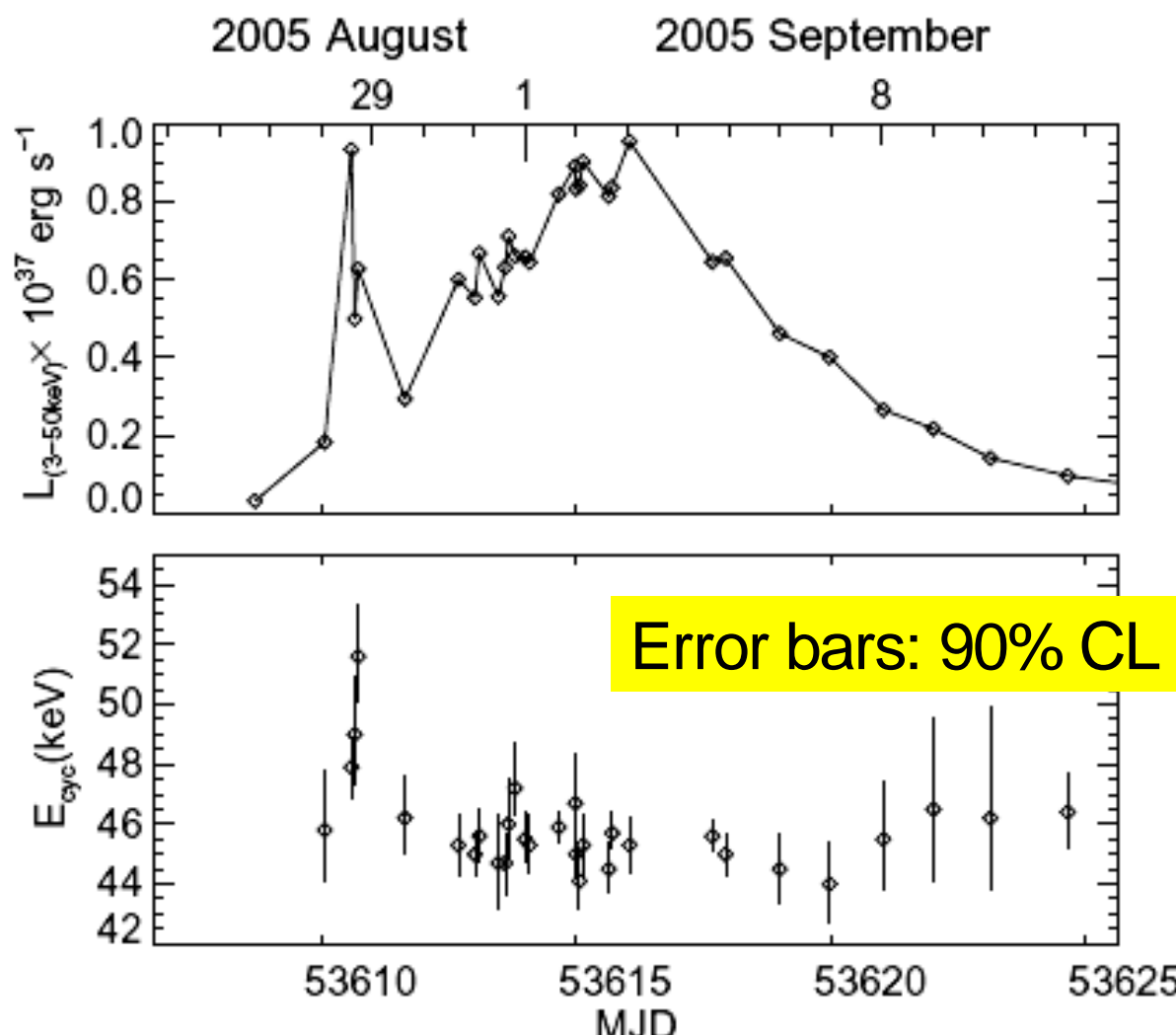
HEXTE A 20.15 – 45.47keV

HEXTE A 45.47 – 91.19keV



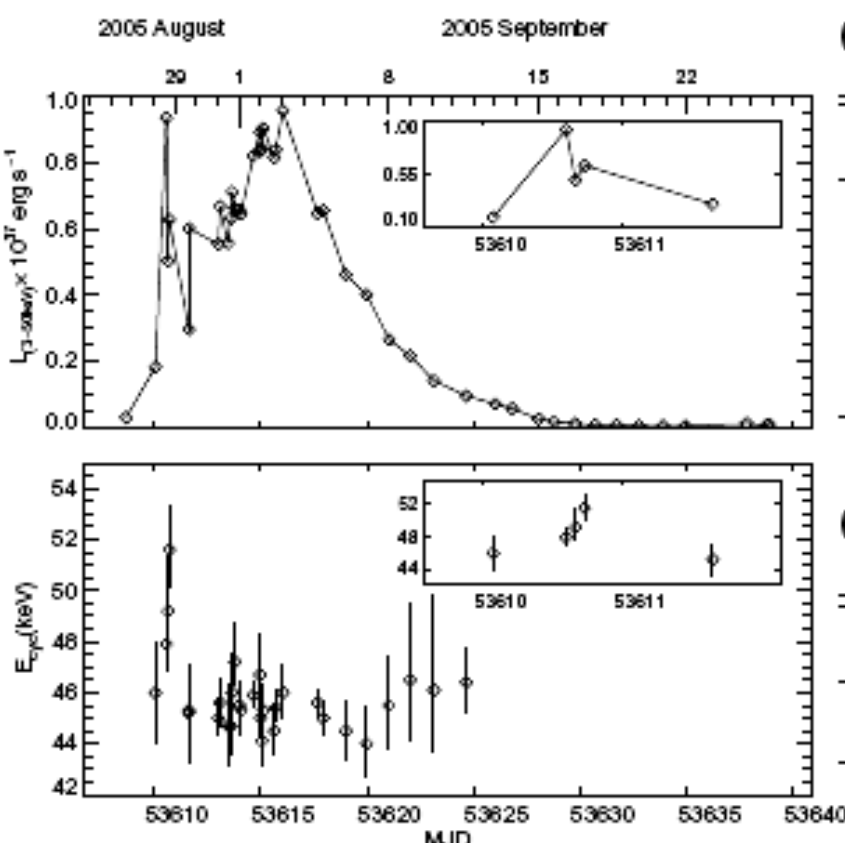
(Caballero et al. 2007, to be submitted)

Spectral evolution - cyclotron energy



Spectral evolution: cyclotron line energy

During the pre-periastron flare the energy of the centroid of the cyclotron line is measured at a higher position



Observations flare

E_{fund} (keV)	$L_{(3-50\text{keV})} \times 10^{37} \text{ ergs}^{-1}$
$47.9^{+1.0}_{-1.0}$	0.94
$49.2^{+2.1}_{-1.6}$	0.50
$51.6^{+1.7}_{-1.5}$	0.63

Obs. close to maximum main outburst

E_{fund} (keV)	$L_{(3-50\text{keV})} \times 10^{37} \text{ ergs}^{-1}$
$45.9^{+0.4}_{-0.3}$	0.82

(errors 90% confidence)

(Caballero et al. 2007, to be submitted)

outburst

pre-flares

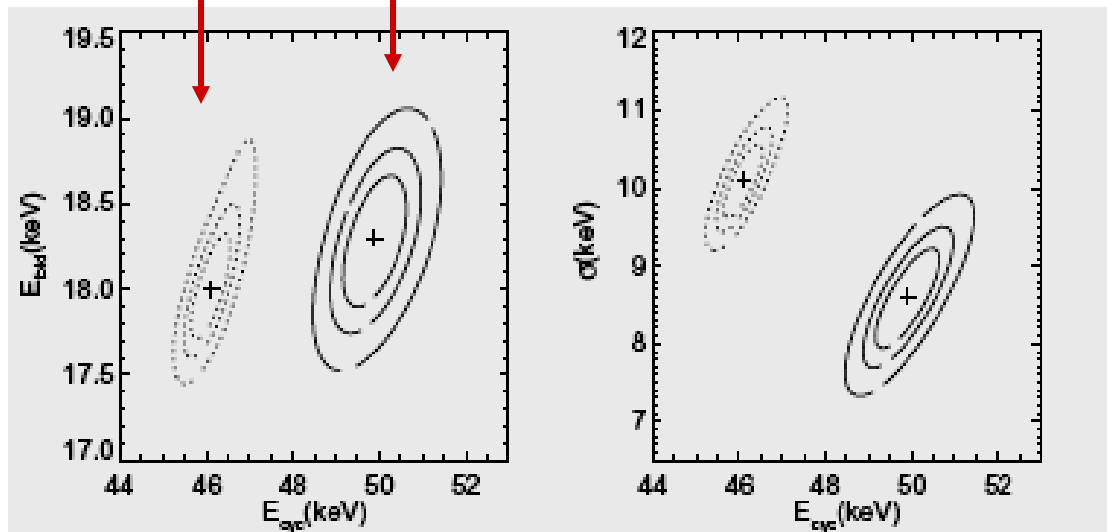
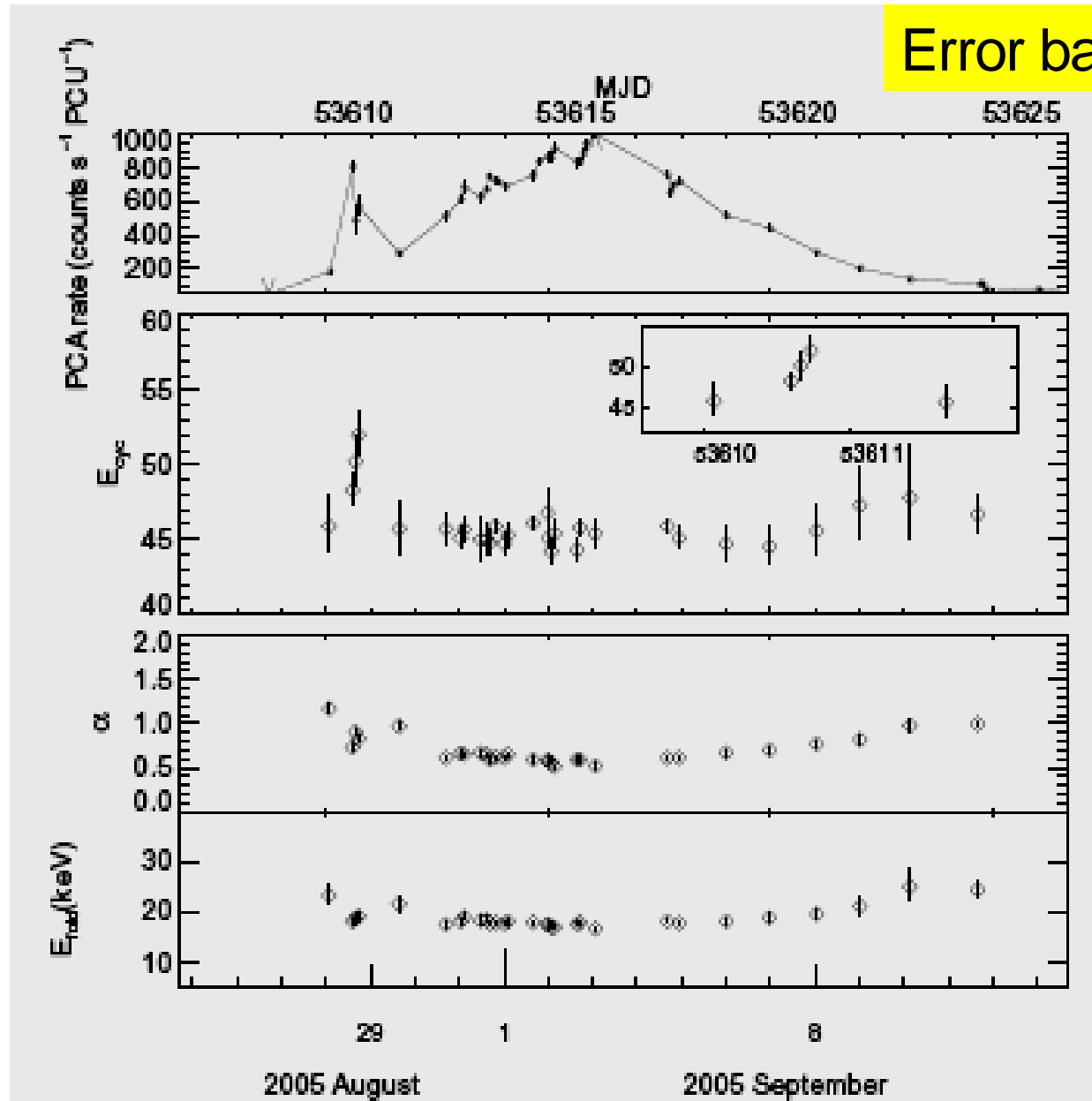


Fig. 3. E_{fold} vs E_{cyc} (left) and σ vs E_{cyc} (right) contour plots for one observation near the maximum (dotted lines, observation (b) in Fig. 2) and for the sum of the three available observations during the pre-outburst flare (solid lines). The contours indicate $\chi^2_{\min} + 2.30(68\%)$, $4.61(90\%)$, $9.21(99\%)$ levels.

Spectral evolution: photon index -cutoff energy

Error bars: 90% CL

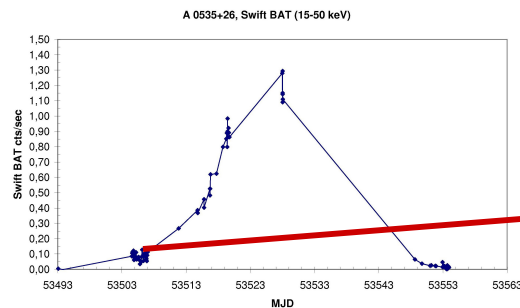


Summary of the RXTE / INTEGRAL analysis

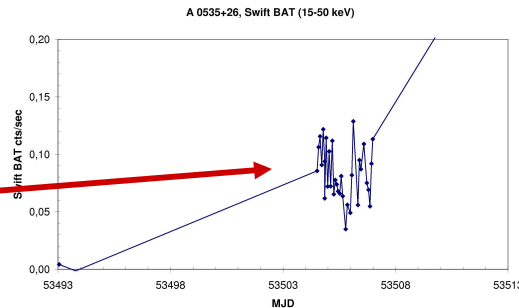
- Fundamental cyclotron line measured at $\sim 45\text{keV}$ with INTEGRAL, RXTE. Result confirmed by Suzaku
- THREE MAIN DIFFERENCES PRE OUTBURST FLARE - MAIN OUTBURST
- Constant period during pre-periastron flare
Spin-up starts at periastron
- Strong pulse profile variation during the pre-periastron flare and the main outburst
- Centroid of cyclotron line higher during the pre-periastron flare, constant during the main outburst

SwiftBAT lightcurves

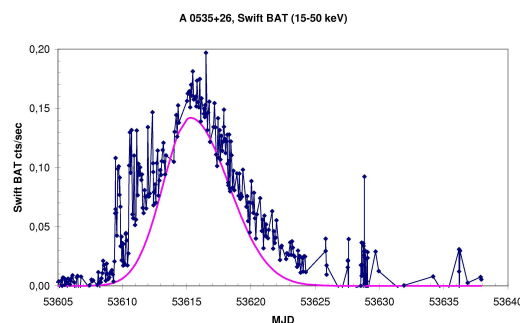
Giant o. Apr/May 05



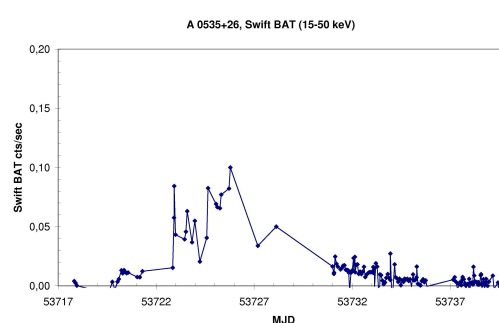
Look-up



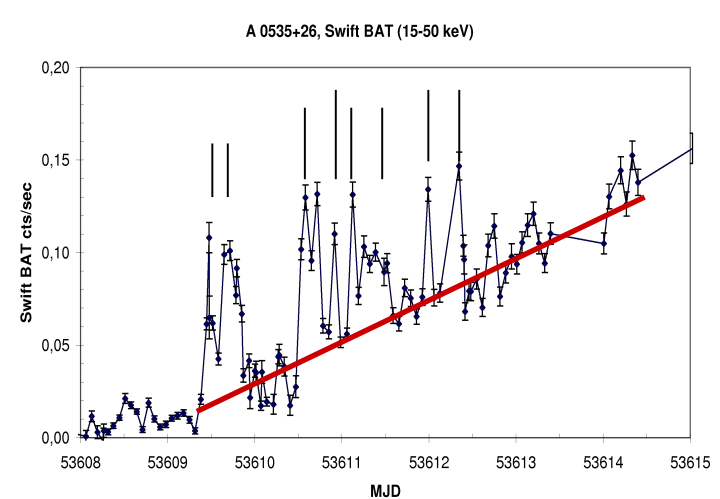
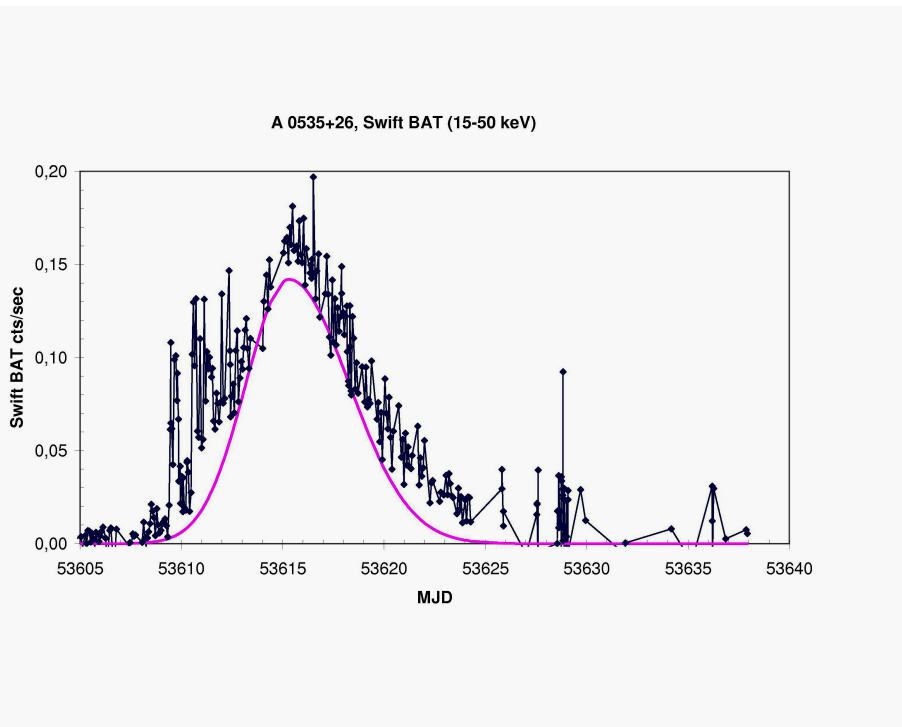
1st normal o. Aug/Sep 05



2nd normal o. Dec 05



Rising of the Aug/Sep 2005 outburst

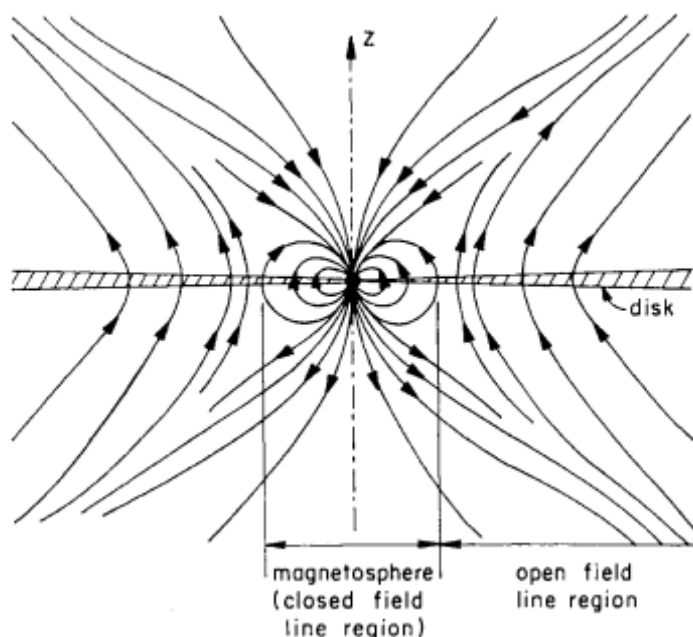


$$\Delta t = 10^4 - 3 \times 10^4 s$$

Typical mass in X-ray flares:

$$\Delta M = \Delta E / (0.1c^2) \approx 10^{20} - 10^{21} g$$

Disk-magnetospheric interaction



Boundary layer:

$<20c_s / \omega_K$ (Anzer & Boerner, 1983)

$\sim 5c_s / \omega_K$ (Lovelace et al. 1995)

Lovelace et al. 1995

Estimate of mass in the boundary layer:

$$\Delta \approx h \sim 0.1 R_m$$

Standard Shakura-Sunyaev accretion disk:

$$\Delta M = \rho (2\pi R_m) \Delta \Delta h ;$$

$$(2 \times 10^{19} \text{ g}) r_{m,9}^{7/5} \alpha^{-4/5} \dot{M}_{-10}^{3/5} (1 - \xi)^{3/5}$$

$$\xi = j / j_{in}, \quad j = \dot{M} \sqrt{GMr}$$

At the beginning of outburst $\xi \approx 0$

$$\alpha \sim 0.01, \dot{M}_{-10} \sim 3 \quad \& \quad M \sim 10^{21} \text{ g}$$

Disc accretion - Magnetospheric instabilities

Development of the instabilities

For low accretion rates,
Kruskal-Schwarzschild
instability can occur:
plasma enters the
magnetosphere in form of
bubbles that fall onto the
NS.

See Postnov et al 2007
Baan 1979
Fig. Arons & Lea 1976

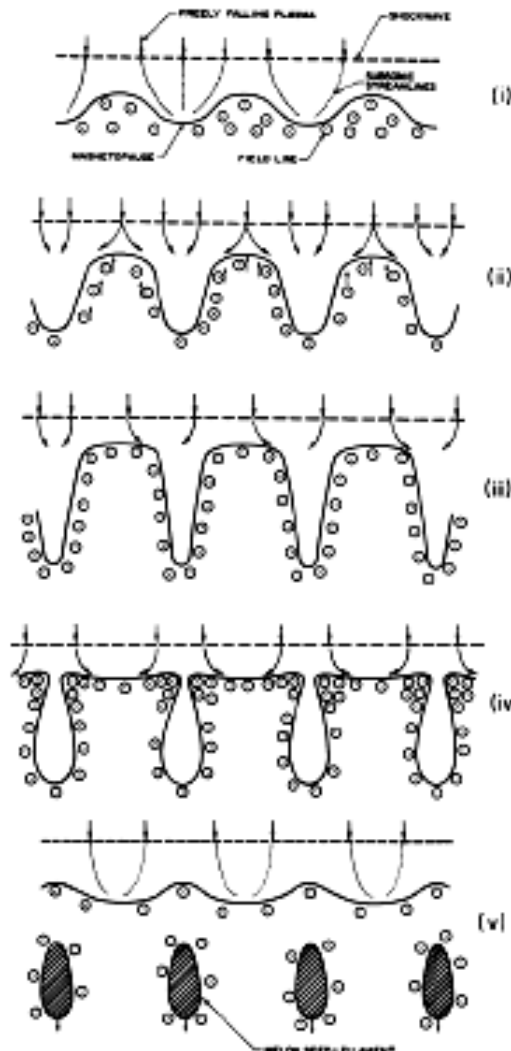


FIG. 4.—Cross section of the development of the interchange instability. (i) Initial nonlinear growth into the hydrostatic layer.

Linear analysis (Arons & Lea, 1976, Baan 1977, 79):

$$\delta\rho : \exp(\Gamma t),$$

$$\Gamma^2 = kg_{eff} \tanh(kz)$$

The effective acceleration near the equatorial plane:

$$g_{eff} \equiv \frac{GM}{r_m^2} - \Omega^2 r_m - \frac{(\mathbf{k} \cdot \mathbf{B} \mathbf{u})^2}{4\pi\rho_m kr_m^6} - \frac{3\mu^2}{4\pi\rho_m R_c r_m^6} - \frac{\delta k \mu^2}{4\pi\rho_m r_m^6} - \frac{\Omega r_m}{4} \left| \frac{dV_\phi}{dz} \right|_{r_m}$$

Centrifug. force

m.f.line curvature

Bending of field lines
due to instability

1st-order correction
due to current sheet

$g_{eff} > 0$ \hookrightarrow instability; low-modes (large k) first unstable

$g_{eff} < 0$ \hookrightarrow stability

At small \dot{M} , accretion is centrifugally prohibited

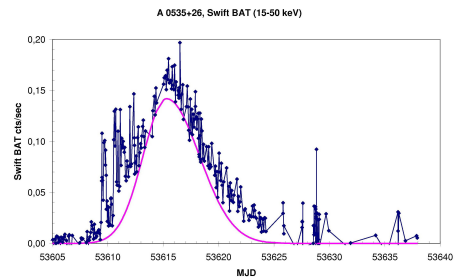
$$(R_m > r_{cor} = (GM / \omega_*^2)^{1/3}). g_{eff} \equiv \frac{GM}{R_m^2} (1 - \omega_*^2 / \omega_K^2) < 0$$

When \dot{M} increases, $R_m \nexists \dot{M}^{-2/7}$ decreases

At the onset of accretion (when $R_m < R_{cor}$) g_{eff} can be positive
unstable magnetospheric accretion can occur
(like in the rapid burster MXB 1730-335)

How does this explain the observed features of Aug/Sep 05 outburst?

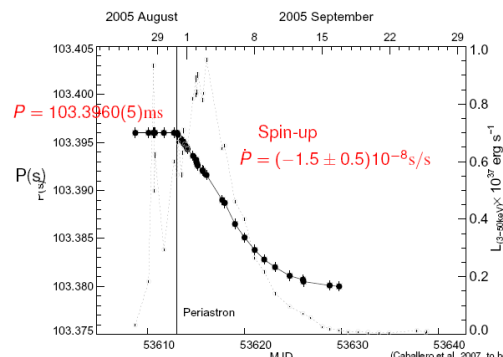
1) X-ray luminosity of flares are due to spasmotic accretion of matter from unstable NS magnetosphere



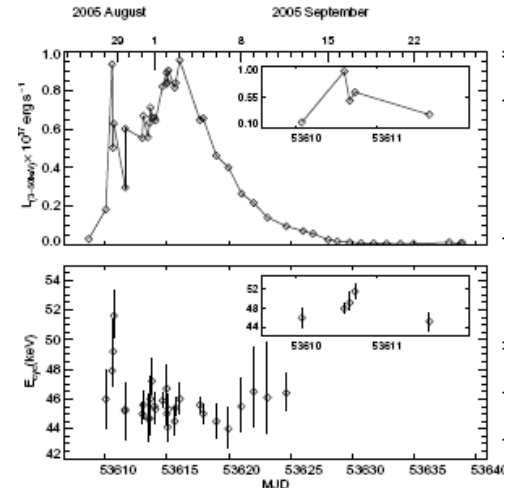
2) Blobs with $\Delta M \approx 10^{21}$ g produce very small spin-up

$$\left| \frac{\Delta P}{P} \right|_{\max} = \frac{\Delta M \sqrt{GMR_m}}{2\pi I} \approx 7 \times 10^{-6},$$

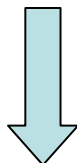
within period measurement errors



3) Plasma entering magnetosphere through KS-instability can be frozen closer to NS and falls along different lines difference in the CRSF in flares and the main outburst



4) Independence of E_c on luminosity during the main outburst suggests the absence of radiation-dominated accretion column (like in Her X-1, Staubert et al. 2007). $\Delta E_c/E_c \sim 10\%$ in the flare $\Delta B/B \sim 10\%$ $\Delta R/R \sim 3\%$ $\Delta R \sim 300 \text{ m}$! Emission during the flare comes almost from the NS surface.

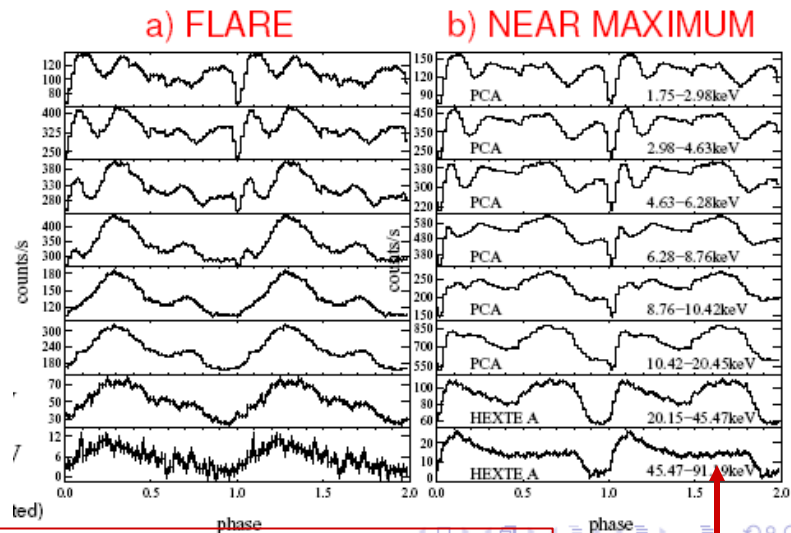
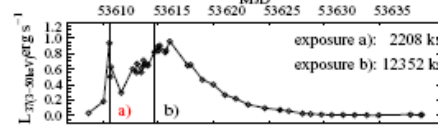


Explanation of the different pulse profile evolution

5) Smooth p.p. change with energy in the flare suggests **pencil-beam** emission diagram in the flares.

In the main outburst accretion column is higher and can have additional **fan-beam** formed by e- photons.

Energy profiles



Only pencil-beam ?

Fan-beam due to e-photons disappears after crossing E_c

$$E = E_c :$$

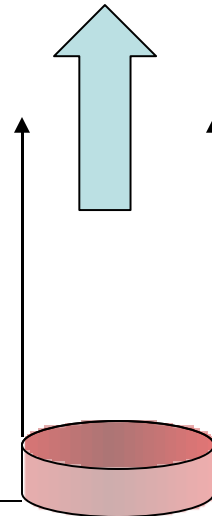
$$\sigma_p ; \sigma_T (E/E_c)^2 \text{ (e)}$$

$$\sigma_{\perp} ; \sigma_T [\sin^2 \theta + \cos^2 \theta (E/E_c)^2]^{1/2} \text{ (o)}$$

¶ $\sigma_p = \sigma_{\perp}$ @ $\theta \sim \pi/2$

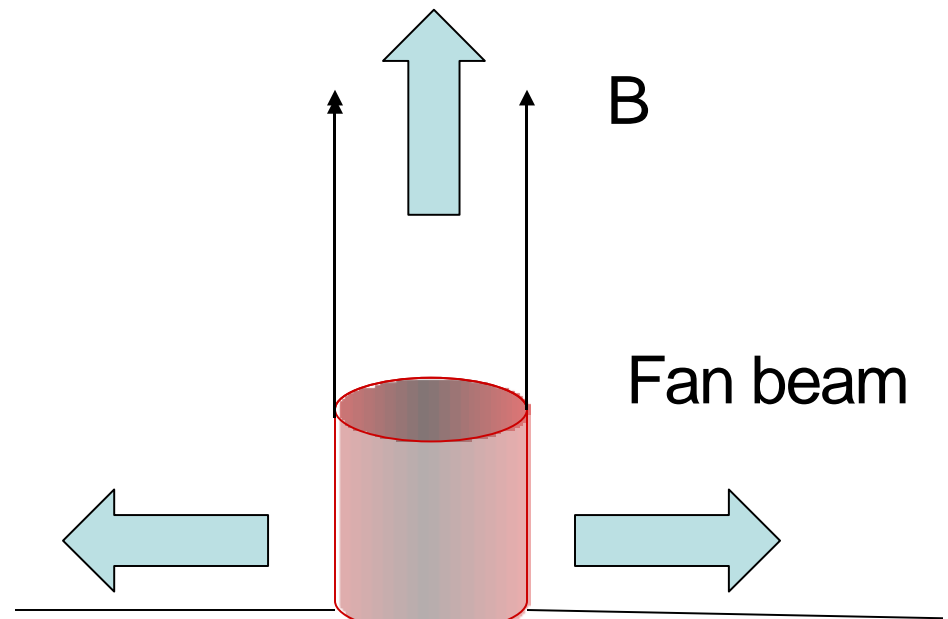
$$E \gg E_c : \sigma_{\perp} \sim \sigma_p @ \theta \sim \pi/2$$

Pencil-beam



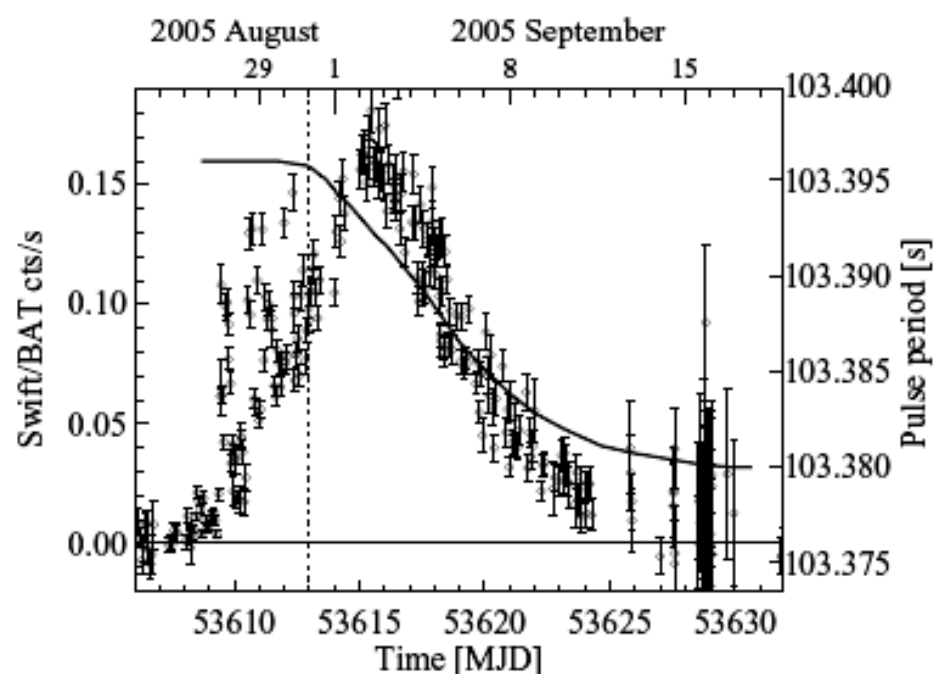
Flares

Pencil-beam

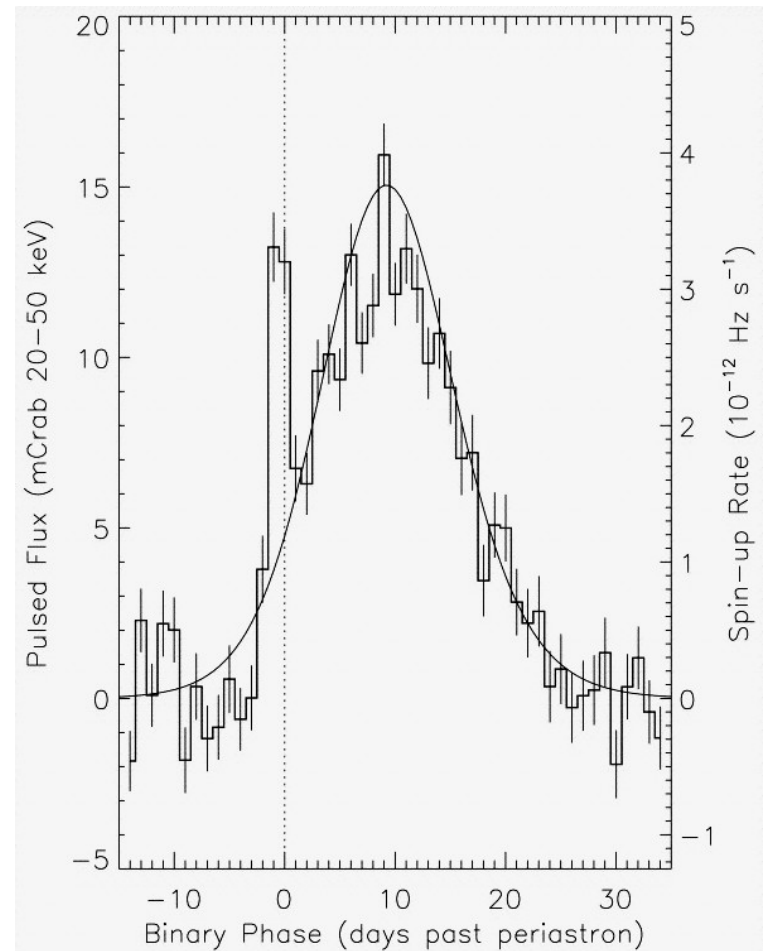
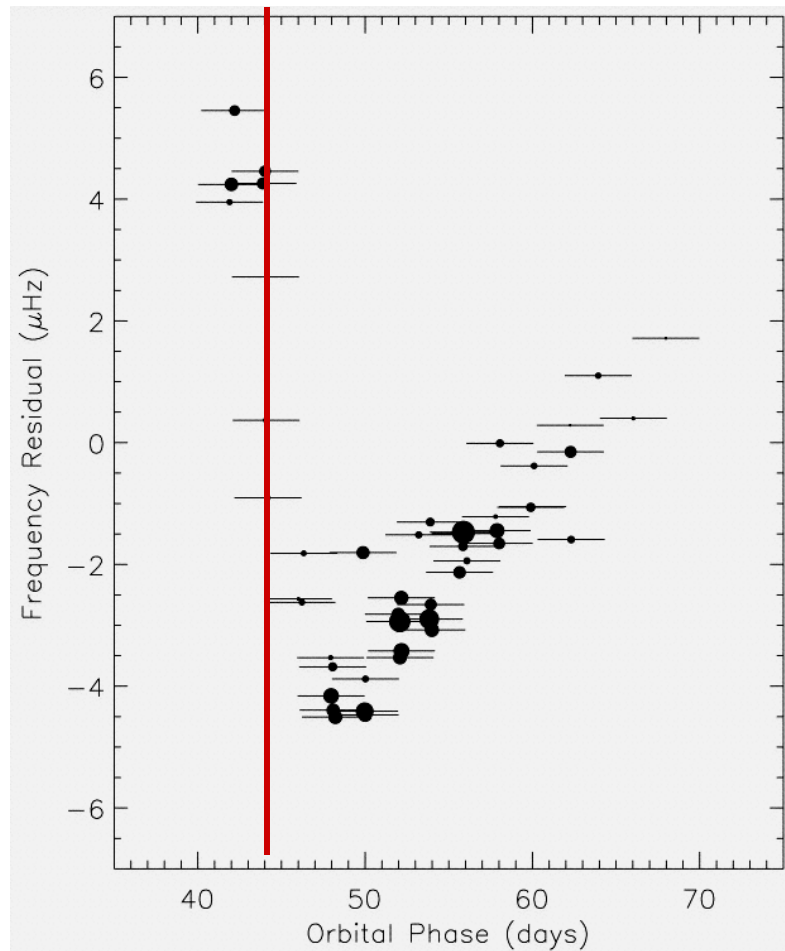


Main outburst

6. The amplitude of X-ray flares are strongly reduced when the NS spin-up starts, because then $\xi = j/j_{in} \rightarrow 1$ and the mass in the boundary layer decreases ($\Delta M \sim (1 - \xi)^{3/5}$). When spin-up stops, flaring activity appears again (after Sep. 14, see the BAT light curve)

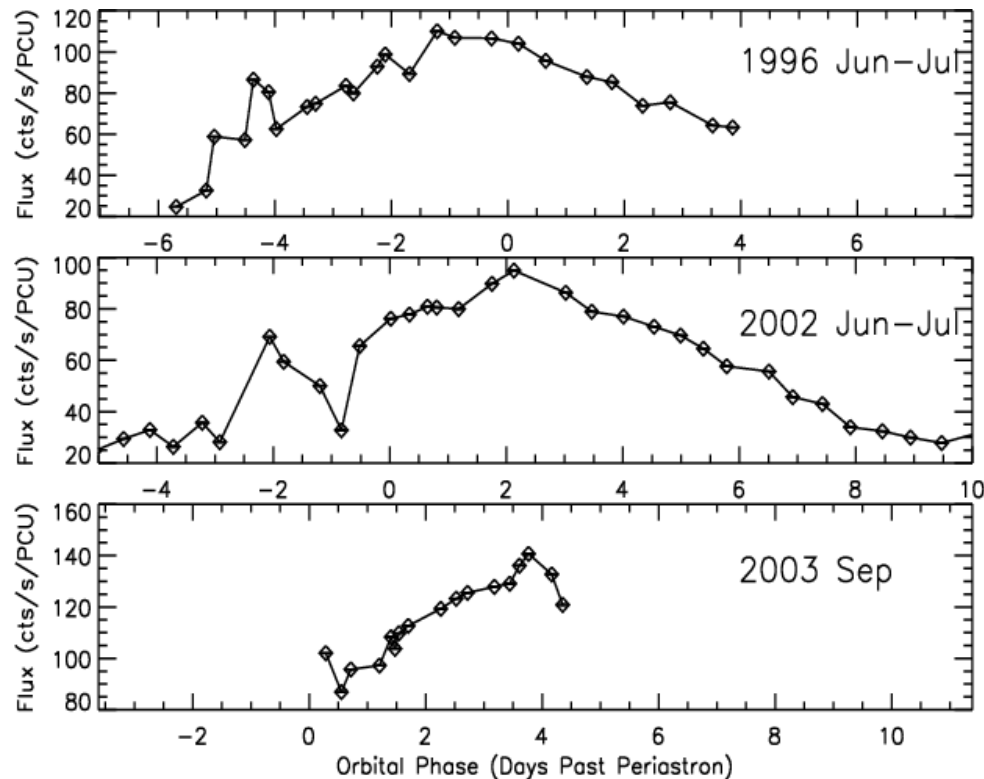
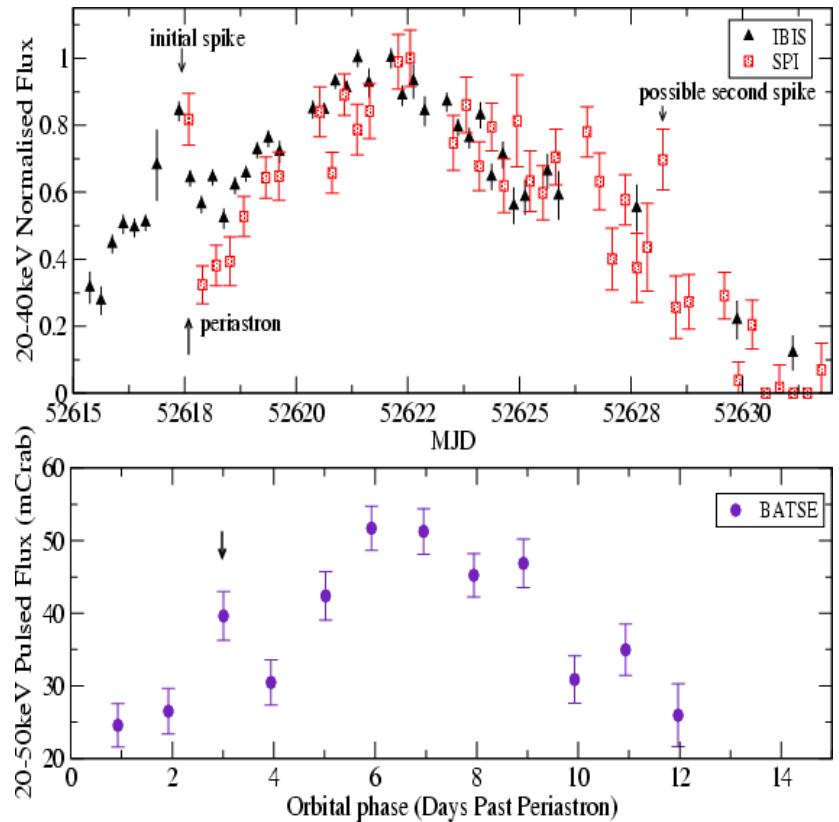


Other X-ray transients: 1) 2S 1845-024



Finger et al. 1999

2) EXO 2030+375



Camero Arranz et al 2005

Conclusions

- X-ray flares at the beginning of X-ray outbursts in A 0535+26 can be due to low-mode magnetospheric instability
- Spasmodic accretion on top of quasi-stationarily increasing accretion rate explains all features observed in Aug/Sep 2005 outburst of A 0535+26
- Such behavior is expected at some critical accretion rate and is observed in other sources (e.g. 2S 1845-024 (Finger et al. 1999), EXO 2030+375 (Cano et al. 2005)).
- Further studies are underway searching for cyclotron line energy in other flares of A 0535+26 and in other sources